Development of the Mechanistic Critical Heat Flux Prediction Methodology for Tube and Annulus Geometries

Min Seo Son [a], Yongsuk Choi [a], Tae Young Yang [a], Gi Won Bae [a], Hyoung Kyu Cho [a*]
[a] *Department of Nuclear Engineering, Seoul National University, 1 Gwanak-ro, Gwanak-gu, Seoul 08826*
[*]Corresponding author: chohk@snu.ac.kr

***Keywords :** critical heat flux, mechanistic model, liquid sublayer dryout, film analysis, regime classification

1. Introduction

Critical Heat Flux (CHF) is a key thermal–hydraulic safety limit in the design and safety criteria of innovative Small Modular Reactor (i-SMR). Reliable CHF prediction over wide operating conditions and channel geometries is essential for SMR safety analyses.

The i-SMR adopts a boron–free core and considers load-following operation. These operation characteristics widen the range of pressure, mass flux, and inlet subcooling, which necessitate a larger CHF database. However, it is difficult to obtain a CHF database that covers the full range of operation conditions required for design and safety assessments. Therefore, a physics-based mechanistic CHF model is required to provide reliable CHF predictions across a wide range of operating conditions.

In this study, a mechanistic CHF prediction framework is developed to improve prediction performance across a broad range of thermal-hydraulic conditions. CHF is generally categorized into departure from nucleate boiling (DNB) and dryout (DO). Individual mechanistic models are applied to each regime because the governing physical mechanisms differ between the two regimes. A regime classification method is also implemented to identify whether a given condition is DNB- or DO-dominant using only the channel geometry and thermal–hydraulic conditions. The proposed framework is validated against experimental CHF data obtained under tube and annulus channels with using a uniform power profile.

2. Mechanistic models

In this section, the mechanistic models employed in this study for CHF prediction are described. For DNB-type CHF prediction, a liquid sublayer dryout model [1~4] is used, and a film analysis model [5~6] is used for DO-type CHF prediction.

2.1 Liquid sublayer dryout model

The liquid sublayer dryout model assumes that DNB-type CHF occurs when a vapor blanket suppresses wall–liquid heat transfer, depleting the thin liquid sublayer beneath the blanket (Fig. 1.). The liquid sublayer dryout model was originally developed by Lee & Mudawar (1988) [1]. In this study, the present implementation follows the Liu (2000) [2] model for tube geometries. For the annulus geometries, the model is established based on the Liu (2022) [3] model and the Yoo (2024) [4] model.

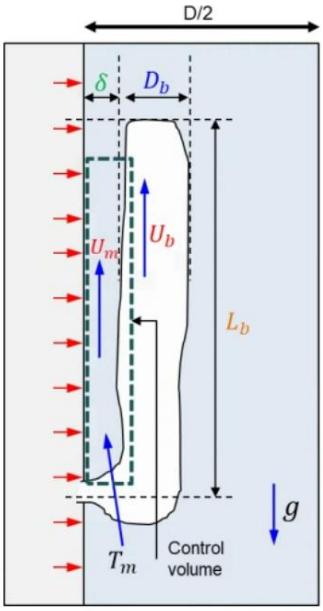

Fig. 1. Schematic diagram of the liquid sublayer dryout model

The CHF is calculated using the formula proposed in Ref. [2].

$$q''_{\mathrm{CHF}} = \rho_{\mathrm{f}} \delta h_{\mathrm{fg}} U_{\mathrm{b}} / L_{\mathrm{b}} \tag{1}$$

where q''_{CHF} (W/m^2) is the critical heat flux, ρ_{f} (kg/m^3) is the density of the liquid, δ (m) is the thickness of the sublayer, h_{fg} (J/kg) is the latent heat, and U_{b}(m/s) is the vapor blanket velocity, and L_{b} (m) is the vapor blanket length.

Vapor blanket length is assumed to be equal to the Helmholtz instability wavelength. [1]

$$L_{\mathrm{b}} = \frac{2\pi\sigma\left(\rho_{\mathrm{f}} + \rho_g\right)}{\rho_{\mathrm{f}}\rho_{\mathrm{g}} U_{\mathrm{b}}^2} \tag{2}$$

where ρ_{g} (kg/m^3) is the density of the gas, σ (N/m) is the surface tension.

Vapor blanket velocity is calculated using the formula proposed in Ref. [4].

$$U_{\mathrm{b}} = \frac{V_{\mathrm{c}}}{1 + \sqrt{\frac{\rho_{\mathrm{c}} + \rho_{\mathrm{g}}}{\rho_{\mathrm{f}} + \rho_{\mathrm{g}}} * \frac{\rho_{\mathrm{f}}}{\rho_{\mathrm{c}}}}} \tag{3}$$

where, $V_c = G/\rho_{\mathrm{c}}$ (m/s) is the bulk liquid velocity, $\rho_{\mathrm{c}} = (1-\alpha)\rho_{\mathrm{lout}} + \alpha\rho_{\mathrm{g}}$ (kg/m^3) is the two-phase bulk liquid density, ρ_{lout} (kg/m^3) is the liquid density at the end of the heated length (EHL), and α is the void fraction.

The sublayer thickness is calculated using the formula proposed in Ref. [1].

$$\delta = y - D_{\mathrm{b}}/2 \tag{4}$$

where y (m) is the distance between the center of the vapor blanket and the wall, and D_{b} is the vapor blanket diameter.

The distance between the center of the vapor blanket and the wall is calculated by using the force balance between the buoyancy and the drag force. [1]

$$U_{\mathrm{bl}} = U_{\mathrm{b}} - \left(\frac{2L_{\mathrm{b}}g(\rho_{\mathrm{f}} - \rho_{\mathrm{g}})}{\rho_{\mathrm{f}}C_{\mathrm{D}}}\right)^{0.5} \tag{5}$$

where U_{bl} (m/s) is the velocity at the center of the vapor blanket, and C_{D} is the drag coefficient.

Once U_{bl} is obtained, the dimensionless distance from the heated wall is determined using the liquid velocity profile correlation corresponding to the tube/annulus geometry. The dimensionless distance is converted to the physical distance (y), and the sublayer thickness is calculated.

The sub-models used to calculate the void fraction, net vapor generation (NVG) point, and the other thermal-hydraulic variables are summarized in Table I.

Table I: Liquid sublayer dryout submodels

Parameter	References
Void fraction	Ahmad (1970) [7]
NVG (water)	Levy (1967) [8]
NVG (non-water)	Saha – Zuber (1974) [9]
Liquid temperature at the EHL	Levy (1967) [8]
Vapor blanket diameter	Levy (1967) [8]
Friction factor (tube)	Colebrook – White (1937) [10]
Friction factor (annulus)	Nouri (1993) [11]
Drag force coefficient	Harmathy (1960) [12]
Liquid velocity profile (tube)	Arpaci & Larsen (1984) [13]
Liquid velocity profile (annulus)	Nouri (1993) [11]

For a given geometry parameters and thermal-hydraulic conditions, the CHF is obtained through an iterative calculation. Convergence is assumed when the relative difference between the computed CHF and the guessed wall heat flux is within 1 %.

2.2 Film analysis model

The film analysis model assumes that DO-type CHF occurs when the liquid film adjacent to the heated surface is completely depleted after the onset of annular flow (Fig. 2.). In the annular flow regime, the liquid phase exists as a liquid film and entrained droplets. The depletion of the liquid film is determined by the competing effects of droplet entrainment, deposition, and liquid film evaporation.

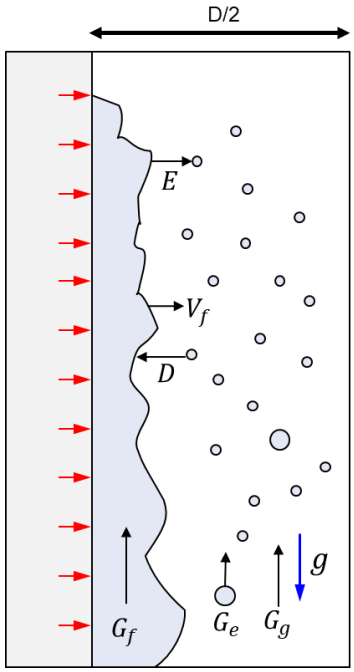

Fig. 2. Schematic diagram of the film analysis model

In this study, the present implementation follows the modified Ahmad (2013) [5] model. For the annulus geometries, the model is established based on Zhang & Hewitt (2016) [6] model.

CHF is calculated by using the axial mass conservation equations. The governing equations are derived under the five assumptions: (1) steady-state, (2) 1D flow, (3) circumferentially uniform film thickness, (4) negligible slip between the vapor and droplets, (5) negligible evaporation from the droplets. [5]

$$Liquid\ film: \frac{\mathrm{d}}{\mathrm{dz}} G_{\mathrm{f}} = \frac{4}{D_{\mathrm{h}}}(D - E - V_f) \quad (6)$$

$$Entrained\ droplet: \frac{\mathrm{d}}{\mathrm{dz}} G_{\mathrm{e}} = \frac{4}{D_{\mathrm{h}}}(E - D) \quad (7)$$

$$vapor: \frac{\mathrm{d}}{\mathrm{dz}} G_{\mathrm{g}} = \frac{4}{D_{\mathrm{h}}} V_f \quad (8)$$

where $G_{\mathrm{f}}, G_{\mathrm{e}}, G_{\mathrm{g}}$ (kg/m^{2}s) is the mass flux of the liquid film, droplet, vapor. D_{h} (m) is the hydraulic diameter, D (kg/m^{2}s) is the deposition rate, E (kg/m^{2}s) is the entrainment rate, $V_{\mathrm{f}} = q''/h_{fg}$ (kg/m^{2}s) is the evaporation rate from the liquid film.

Boundary conditions are specified at the onset of annular flow (OAF). The churn-to-annular flow transition point is determined using the Wallis (1969) [14] criterion. The initial entrainment fraction (IEF) at the OAF is another key boundary condition. In the present implementation, a constant value of IEF = 0.7 is used for the tube geometry. For the annulus geometry, IEF = 0.7 is applied for G < 2000, while IEF = 0.8 is used for G ≥ 2000. Also, the liquid film mass flux per unit wetted perimeter is identical on the inner and outer walls at the annulus geometry. Accordingly, the ratio of the outer-to-inner film mass flux is given by the perimeter ratio.

To close the conservation equations, empirical closure relations are used. For the tube geometry, the deposition and entrainment rate model from Okawa & Kataoka (2005) [15] was used. For the annulus geometry, the deposition and entrainment rate model from Hewitt & Govan (1990) [16] was used.

To calculate the CHF, the vapor quality at the OAF is first determined, and the initial mass flux on the walls is obtained using the IEF. The heat flux is increased iteratively, and CHF is determined when either the inner or the outer wall film mass flux reaches zero at any axial location.

3. Regime classification method

In this section, a regime classification method is presented to determine the CHF type (DNB, DO) using the specified channel geometry and thermal-hydraulic conditions.

In this study, the CHF regime is classified using a combined criterion based on the Katto number ($\sigma\rho_{\mathrm{f}}/G^2 l_h$) and the critical quality, where l_{h} denotes the heated length. When the Katto number is 2e-7 or lower, the majority of the experimental data exhibit a critical quality of -0.1 or lower. Therefore, the CHF is directly classified as DNB. In contrast, when the Katto number is 2e-4 or higher, most cases have a critical quality of 0.1 or higher, and the CHF is directly classified as DO.

For the intermediate range between these two thresholds, it is classified into a transition regime, and an additional classification step is required. Two CHF predictions are obtained from the liquid sublayer dryout model and the film analysis model, respectively. The smaller CHF is selected to calculate the critical quality at the CHF location. If the critical quality is lower than -0.1, the CHF is classified as DNB, and the liquid sublayer dryout model (DNB-based mechanistic model) is adopted. If the critical quality is higher than 0.1, the CHF is classified as DO, and the film analysis model (DO-based mechanistic model) is adopted. If the critical quality is between -0.1 and 0.1, the CHF is calculated by interpolating DNB and DO CHF using a sigmoid-based interpolation function. The overall regime classification procedure is summarized as a flowchart in Fig. 3.

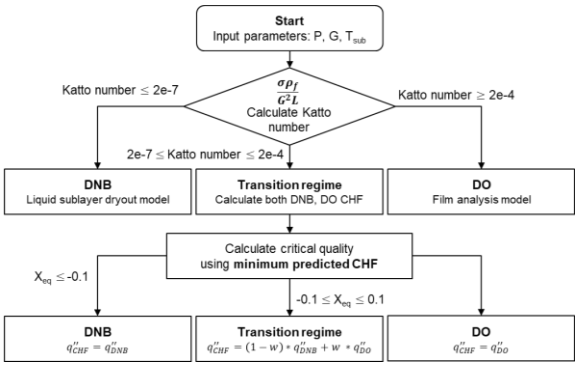

Fig. 3. Flowchart of regime classification method

4. Assessment of the mechanistic model

In this section, the proposed mechanistic model is evaluated for tube and annulus geometries under a uniform power profile using the 2006 Lookup Table (LUT) CHF database [17] and the SNU CHF database, which was constructed by integrating accessible annulus CHF data.

4.1 Tube

To validate the proposed model for tube geometry, an assessment was conducted using the LUT CHF database. The evaluation dataset was selected to cover the operating conditions of i-SMR, including pressure of 11.3 ~ 17.3 MPa, mass flux of 400 ~ 2050 kg/m^{2}s, and inlet temperature of 200 ~ 300 ºC. Prior to applying the regime classification method, the prediction capability of each individual mechanistic model is summarized in Fig. 4.

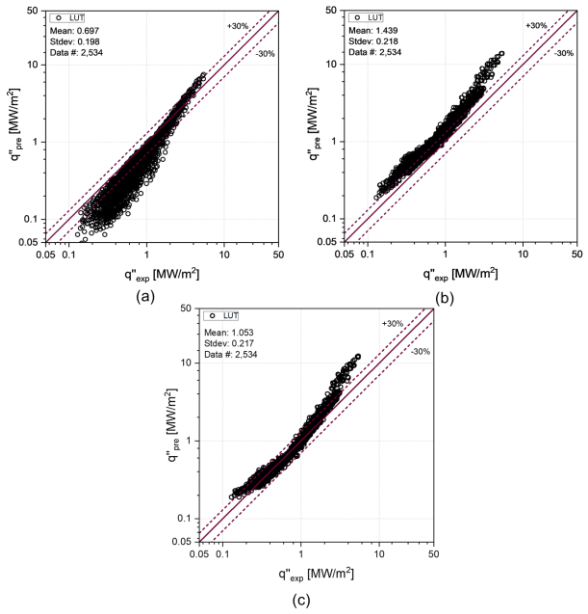

Fig. 4. Comparison of predicted versus experimental CHF at tube (a) liquid sublayer dryout model (b) film analysis model (Ahmad, 2013), (c) film analysis model (this study)

As shown in Fig. 4, the liquid sublayer dryout model shows underprediction for some CHF data. In addition, the baseline film analysis model of Ahmad (2013) shows overprediction for most CHF data. To mitigate this overprediction, the present study modifies the entrainment-deposition model, which enhances the prediction capability of the film analysis model. To further examine the reason of prediction errors in the two models, Fig. 5 presents a comparison between the experimental critical quality and the prediction-to-measurement ratio.

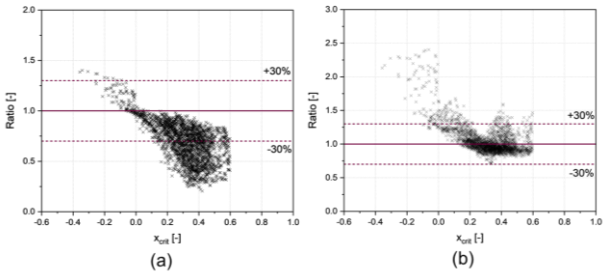

Fig. 5. Comparison of experimental critical quality and prediction-to-measurement ratio (a) liquid sublayer dryout model (b) film analysis model

As shown in Fig. 5, the liquid sublayer dryout model tends to underpredict CHF in the DO-dominant region (critical quality > 0.1), whereas the film analysis model tends to overpredict CHF in the DNB-dominant region (critical quality < 0). This suggests that prediction capability can degrade when each mechanistic model is applied to a different CHF regime. Therefore, applying a regime classification method based on the given geometric and thermal–hydraulic conditions and selecting the corresponding model is expected to improve prediction capability. The comparison results obtained using this methodology are presented in Fig. 6.

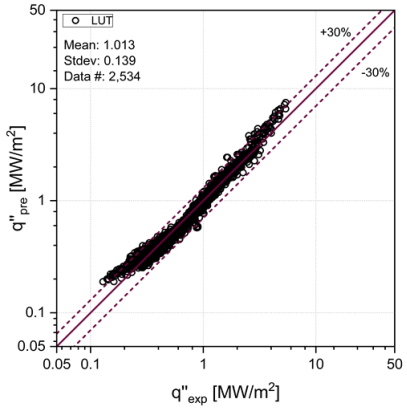

Fig. 6. Comparison of predicted versus experimental CHF for tube using regime classification method

The proposed model achieved a mean prediction-to-experiment ratio of 1.013 with a standard deviation within 13.9%, indicating good prediction capability.

4.2 Annulus

To validate the proposed model for annulus geometry, the assessment was conducted using the SNU CHF database, which includes only internally heated annulus CHF experiments. The evaluation dataset was selected to cover a wide range of thermal-hydraulic conditions: pressure: 0.1 ~ 15.5 MPa, mass flux: 19 ~ 2500 kg/m^{2}s, inlet temperature: 10 ~ 310 ºC, working fluid: R113, R12, R134a, and water. Prior to applying the regime classification method, the prediction capability of each individual mechanistic model is summarized in Fig. 7.

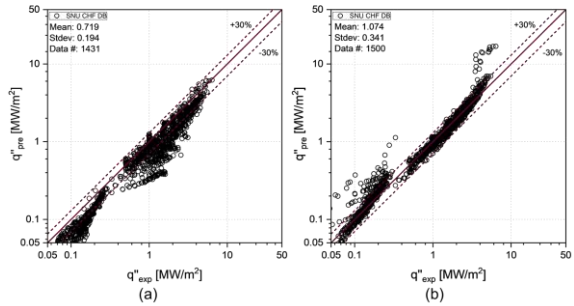

Fig. 7. Comparison of predicted versus experimental CHF at annulus (a) liquid sublayer dryout model (b) film analysis model

Consistent with the tube geometry, the liquid sublayer dryout model tends to underpredict CHF for some CHF data, whereas the film analysis model tends to overpredict CHF for some conditions. Further examination based on the experimental critical quality confirms that prediction capability can degrade when

each mechanistic model is applied to a different CHF regime. Accordingly, a regime classification method is applied to select the appropriate model for each condition, and the comparison result is presented in Fig. 8.

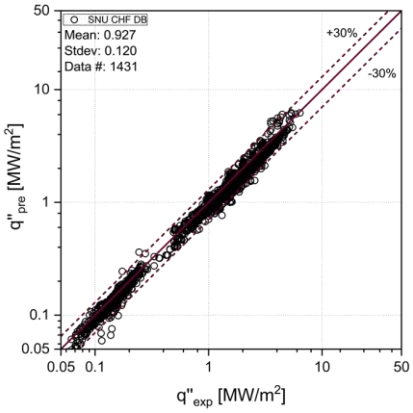

Fig. 8. Comparison of predicted versus experimental CHF for annulus using regime classification method

The proposed model achieved a mean prediction-to-experiment ratio of 0.927 with a standard deviation within 12.0%, indicating good prediction capability.

5. Conclusions

A mechanistic CHF prediction methodology applicable to both tube and annulus geometries was developed by combining a liquid-sublayer dryout model for DNB-type CHF and a film analysis model for DO-type CHF. A regime classification procedure was implemented to select the appropriate CHF mechanism using the Katto number and critical quality-based criterion.

For tube geometry which includes the i-SMR operation conditions, the modified film-analysis model significantly reduced the overprediction observed in the baseline Ahmad (2013) model. For both tube and annulus geometries, the liquid sublayer dryout model underpredicts CHF inferred to be DO-type, whereas the film analysis model overpredicts CHF inferred to be DNB-type. When the regime classification method is applied, the proposed framework achieves good prediction capability regardless of flow-channel geometry. Future work will focus on extending validation to non-uniform power profiles and rod-bundle geometries.

REFERENCES

[1] C. H. Lee and I. Mudawwar, A Mechanistic Critical Heat Flux Model for Subcooled Flow Boiling Based on Local Bulk Flow Conditions, International Journal of Multiphase Flow, Vol. 14, No. 6, pp. 711–728, 1988.
[2] W. Liu et al., Prediction of Critical Heat Flux for Subcooled Flow Boiling, International Journal of Heat and Mass Transfer, Vol. 43, pp. 3371–3390, 2000.
[3] W. Liu, Prediction of Critical Heat Flux for Subcooled Flow Boiling in Annulus and Transient Surface Temperature Change at CHF, Fluids, Vol. 7, No. 7, p. 230, 2022.
[4] J. S. Yoo, Experimental Investigation on Critical Heat Flux of Flow Boiling in an Annulus Channel under Heaving Conditions, Ph.D. dissertation, Dept. of Nuclear Eng., Seoul National Univ., Seoul, Republic of Korea, 2024.
[5] M. Ahmad et al., Phenomenological Modeling of Critical Heat Flux: The GRAMP Code and Its Validation, Nuclear Engineering and Design, Vol. 254, pp. 280–290, 2013.
[6] H. Zhang and G. F. Hewitt, Phenomenological Modelling of CHF in Annular Flow in Annuli Using New Models of Droplet Deposition and Entrainment, Nuclear Engineering and Design, Vol. 305, pp. 284–292, 2016.
[7] S. Y. Ahmad, Axial Distribution of Bulk Temperature and Void Fraction in a Heated Channel with Inlet Subcooling, Journal of Heat Transfer, Trans. ASME, Vol. 92, pp. 595–609, 1970.
[8] S. Levy, Forced Convection Subcooled Boiling Prediction of Vapor Volumetric Fraction, International Journal of Heat and Mass Transfer, Vol. 10, pp. 951–965, 1967.
[9] P. Saha and N. Zuber, Point of Net Vapor Generation and Vapor Void Fraction in Subcooled Boiling, in Proc. 5th Int. Heat Transfer Conf., Tokyo, Japan, Sep. 3–7, pp. 175–179, 1974.
[10] C. F. Colebrook and C. M. White, Experiments with Fluid Friction in Roughened Pipes, Proceedings of the Royal Society of London. Series A—Mathematical and Physical Sciences, Vol. 161, No. 906, pp. 367–381, 1937.
[11] J. M. Nouri et al., Flow of Newtonian and Non-Newtonian Fluids in Concentric and Eccentric Annuli, Journal of Fluid Mechanics, Vol. 253, pp. 617–641, 1993.
[12] T. Z. Harmathy, Velocity of Large Drops and Bubbles in Media of Infinite and Restricted Extent, AIChE Journal, Vol. 6, pp. 281–288, 1960.
[13] V. S. Arpaci and P. S. Larsen, Convection Heat Transfer, Prentice-Hall, Edgewood Cliffs, N.J., 1984.
[14] G. B. Wallis, One-Dimensional Two-Phase Flow, McGraw-Hill, New York, 1969.
[15] T. Okawa and I. Kataoka, Correlations for the Mass Transfer Rate of Droplets in Vertical Upward Annular Flow, International Journal of Heat and Mass Transfer, Vol. 48, No. 23–24, pp. 4766–4778, 2005.
[16] G. F. Hewitt and A. H. Govan, Phenomenological Modelling of Non-Equilibrium Flows with Phase Change, International Journal of Heat and Mass Transfer, Vol. 33, No. 2, pp. 229–242, 1990.
[17] D. C. Groeneveld, Critical Heat Flux Data Used to Generate the 2006 Groeneveld Lookup Tables (NUREG/KM-0011), United States Nuclear Regulatory Commission, Rockville, MD, USA, 2019.